Generation of Chemical Concentration Gradients in Mobile Droplet Arrays via Fragmentation of Long Immiscible Diluting Plugs

ARTICLE *in* ANALYTICAL CHEMISTRY · JANUARY 2013

Impact Factor: 5.64 · DOI: 10.1021/ac303526y · Source: PubMed

2 AUTHORS:

Meng Sun
Texas Tech University
13 PUBLICATIONS **234** CITATIONS
SEE PROFILE

Siva Vanapalli
Texas Tech University
26 PUBLICATIONS **227** CITATIONS
SEE PROFILE

analytical chemistry

Technical Note

pubs.acs.org/ac

Generation of Chemical Concentration Gradients in Mobile Droplet Arrays via Fragmentation of Long Immiscible Diluting Plugs

Meng Sun* and Siva A. Vanapalli*

Department of Chemical Engineering, Texas Tech University, Lubbock, Texas 79409, United States

Supporting Information

ABSTRACT: We report a one-step passive microfluidic technique to generate arrays of moving droplets containing variation of chemical concentration between individual drops. We find that a concentration gradient can be established in a long diluting plug by on-chip dilution and extraction of samples via orthogonal coalescence of the plug with a static array of sample drops. The diluting plug containing the gradient is subsequently fragmented by a droplet generator. We show that the technique is flexible, as the dilution range can be tuned by a variety of control parameters including the carrier fluid flow rate, volume of diluting plugs, and stationary drops. We also find that the concentration gradients have a fine resolution and are reproducible to within 2% relative standard deviation. As one demonstrative application, we show the suitability of the technique for generating a dose-response curve for an enzyme inhibition assay. Because of the ability to inject multiple plugs, our technique has the potential for unlimited as well as sequential dilution of a series of substrates. Thus, our method could be valuable as a high-throughput and high-resolution screening tool for assays that require interrogation of the response of one or more target species to numerous distinct chemical concentrations.

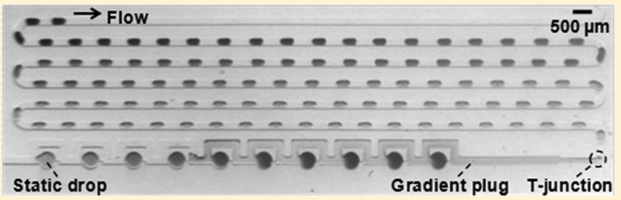

Droplet-based microfluidics[1−5] is emerging as an effective tool for conducting high-throughput chemical and biological analysis by confining analytes inside oil-isolated aqueous droplets. The reduced possibility of cross contamination between the individual droplet containers have been particularly utilized for screening applications ranging from protein crystallization[6−8] to enzyme reaction kinetics[9−12] to cytotoxicity testing.[13−15] In these applications, it is essential to interrogate the response of the compartmentalized analytes to varying concentrations of a reagent. As a result, there is growing interest to develop techniques to generate chemical concentration gradients in microfluidic droplet arrays. Currently, such concentration gradients are being developed in either static or mobile format. Generating concentration gradients in static droplet arrays (SDAs)[16−19] is beneficial for reactions that require long-term observation but could be limited in throughput because of the need for a larger device foot print. Alternatively, manipulating concentration gradients in mobile droplet arrays (MDAs) is well suited for reactions of short time-scale and is amenable to higher throughput.

Concentration gradients in MDAs have been previously achieved by adjusting the flow rates of sample and buffer streams that feed into a droplet generator.[9,10] This approach relies substantially on the stability of flow generated by syringe pumps and yields a concentration range that spans 2 orders of magnitude. Other methods for generating concentration gradients in MDAs are based on sample diffusion or dispersion in single-phase flows. In a diffusion-based gradient generator, a tree-like microfluidic network[20,21] is used to stabilize coflowing laminar streams of sample and buffer, allowing sample molecules to diffuse laterally across the channel to form the concentration gradient. An immiscible phase is introduced downstream to compartmentalize the gradient streams into droplets.[22,23] For these platforms, the range of reagent concentration is quite limited because the design of the microfluidic channel network becomes increasingly complex with the number of distinct concentrations desired. In techniques utilizing Taylor-Aris dispersion, a sample zone is introduced into a stream of buffer to generate a concentration gradient along the flow direction in a microfluidic channel, which is subsequently compartmentalized into droplets.[11,12,24−26] The balance between sufficient dispersion of sample to achieve a low concentration and preventing too much dilution to preserve the original concentration of the sample may limit the range of concentration gradient, which can be alleviated by injecting an extremely long sample plug (e.g., 50 cm in ref 11).

Distinct from the methods based on single-phase flows, techniques relying on coalescence and mixing between droplets generated by drop-on-demand generators have also been exploited to create concentration variation in MDAs.[27−29] In these active approaches, both the drop volumes and coalescence need to be precisely controlled and coordinated by integrated electrodes or valves, and the concentration range demonstrated was about 2 orders of magnitude. More recently, a passive method[30] which induced head-on coalescence between a stationary sample drop and a train of buffer droplets

Received: December 5, 2012
Accepted: January 10, 2013
Published: January 10, 2013

   dx.doi.org/10.1021/ac303526y | *Anal. Chem.* 2013, 85, 2044−2048

has been reported to yield 4 orders of magnitude of concentration using ~30 diluting droplets. This technique is attractive because of the access to a wider concentration range; however, the logarithmic nature of dilution precludes high resolution screening from a multitude of drops.

In contrast to prior methods, here we report a new method based on a unique physical principle for gradient generation. Our technique produces a concentration gradient in a long moving plug by sequentially extracting on-chip samples, allowing partial mixing of sample with water inside the plug, and followed by fragmentation of the gradient plug into chemically distinct droplets. Compared to prior two-phase techniques, we show our method offers the following distinct advantages: (i) the dilution range of concentration can be tuned by various control parameters including plug flow rate and the volumes of stationary drops and moving plugs, lending flexibility to our method; (ii) multiple diluting plugs can be delivered in one step, thereby enabling unlimited dilution of the original sample; (iii) a competitive throughput of at least 6500, 10 nL droplets per hour with fine resolution over the concentration; (iv) the ability to replace prestored sample drops and perform sequential dilutions, thereby enabling screening of multiple targets. Finally, we demonstrate that the MDA with concentration gradient can be further manipulated by mixing with other reagents for determining half maximal inhibitory concentration (IC_{50}) in an enzyme inhibition assay.

EXPERIMENTAL SECTION

Device Design. Figure 1A shows the mask design of the microfluidic device, which mainly contains three parts: (I) a series of ten identical loops for storage of sample drops and generation of concentration gradient in a diluting plug. Each loop contains a bypass channel having lower hydrodynamic resistance than the branch containing the fluidic trap. The width and length of the bypass channel are 200 μm and 2.03 mm, respectively. The diameters of the trap we used are 450, 320, and 200 μm, with the same dimension of the constriction channel (40 μm wide and 100 μm long). The channel height is kept constant at 200 μm. The hydrodynamic resistance ratio (R_B/R_T) of the bypass channel (R_B) and lower branch (R_T) is 3.2 according to the exact analytical solution of Poiseuille flow in a rectangular channel.[31] (II) A T-junction for fragmentation of the long moving plug into mobile droplets with varying concentrations. (III) A reagent channel for injection of a fixed concentration of reagent into a train of chemically distinct droplets. Descriptions of device fabrication, materials, and equipment are provided in the Supporting Information.

Basic Description of the Method. Figure 1B illustrates our chemical gradient generation method with a representative experiment using black dye as sample (see also Movie S1 (ac303526y_si_002.avi), Supporting Information). To perform this experiment, we built a cartridge[6,19] containing sample plug and diluting (water) plug, separated by oil. The plugs are delivered into the microfluidic device through the sample introduction channel using a single pump and syringe.

Sample plug comes first (Figure 1B-i), and it is uniformly divided as it traverses the microfluidic network forming a SDA (in gradient generation region, Figure 1B-ii), according to the flow-resistance mechanism described previously.[19,32] The subsequent diluting plug flows past the stationary drops and exchanges water for sample after the oil film sandwiched between the two aqueous phases breaks inducing coalescence (Figure 1B-iii). This coalescence event pushes water from the

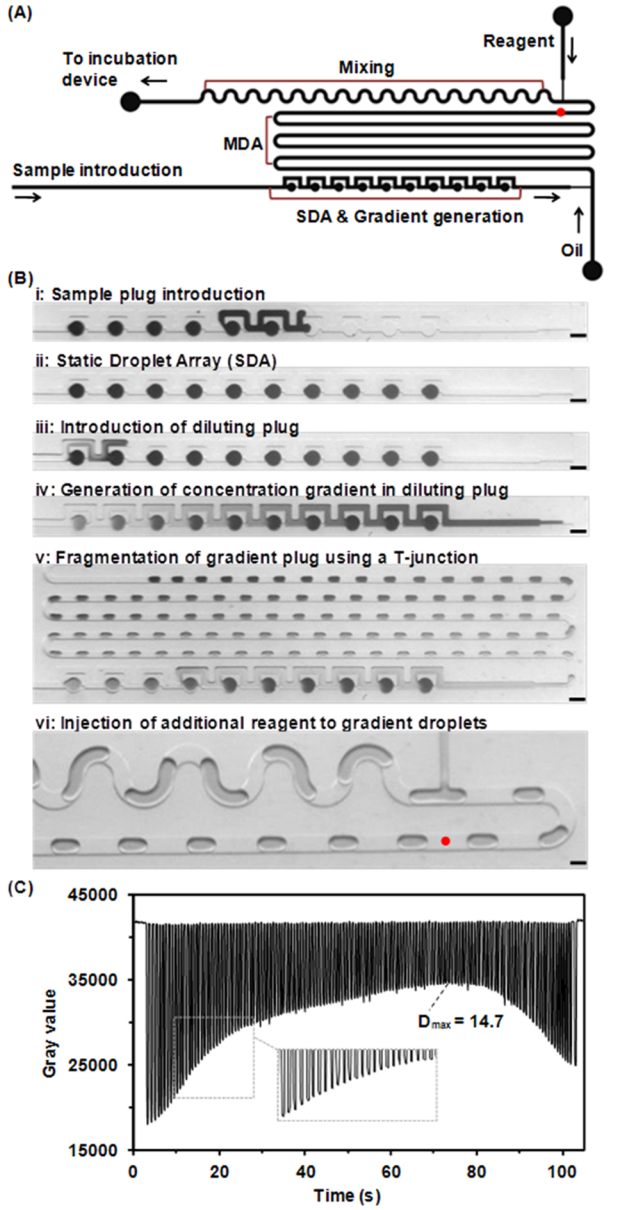

Figure 1. Generation of concentration gradient in MDAs. (A) Schematic design of the microfluidic device: the red dot indicates the location where concentration of sample was measured in the mobile droplets. (B) Snapshots taken in a representative experiment using black dye as sample. Oil flow rates for pushing and fragmenting the diluting plug are 60 and 100 μL/h, respectively. Reagent injection flow rate: 50 μL/h. Volumes of sample and diluting plug: 0.3 and 1.5 μL. Trap size is 450 μm. Scale bar is 500 μm in (i–v) and 200 μm in (vi). (C) Gray-scale intensity values of the gradient droplets generated in panel B-v.

diluting plug into the sample drop, and at the same time, sample is transported into the head of the moving plug. Additional sample is advected during the entire period when the stationary drops and moving plug are in contact. Sample mixing also simultaneously occurs because of dispersion and fluid recirculation in the long moving plug. This process of fluid exchange, advection, and mixing repeatedly occurs as the diluting plug keeps coalescing with stationary drops. As a result, most of the extracted sample gets accumulated at the head of the plug, producing a high sample concentration at its front. However, a decreasing amount of sample is present along the

dx.doi.org/10.1021/ac303526y | Anal. Chem. 2013, 85, 2044–2048

length of the diluting plug, due to less effective mass transfer during the advection period. Thus, a sample concentration gradient is established in the diluting plug (Figure 1B-iv).

We note that the sample concentration is highest at the front of the plug and keeps decreasing along the plug and then could increase again at the tail of the moving plug. The increase is because, during the break-up of the tail of the plug with the stationary drop, an anticlockwise stirring flow (Movie S3 in ref 19) is induced inside the drop, which can sweep extra sample out of the drop (as long as there is enough sample left in the drops), as observed in the tail of the plug in Figure 1B-v. The developed gradient is compartmentalized into droplets by introducing a carrier fluid orthogonal to the direction of moving plug. The sample concentration preserved in individual droplets is determined by analyzing the variation in gray scale values using a custom-written MATLAB routine (see details in Supporting Information) and captured in Figure 1C as a concentration gradient profile. Additionally, to characterize the gradient, we define the maximum dilution fold (D_{max}) as the ratio of the starting concentration of dye in the SDA prior to injecting the diluting plug (which is known a priori) to the minimum concentration detected in the MDA (derived from the calibration curve in Figure S1, Supporting Information). Other downstream manipulations[33−35] can be performed with the MDA, for example, as shown in Figure 1B-vi, where we merge the gradient droplets with a fixed concentration of a reagent, mimicking the need in screening applications where dose response curves are generated by exposing a target species to varying concentration of a reagent.

RESULTS AND DISCUSSION

Performance of the Dilution Technique. Several experimental parameters can be used to control the concentration range in MDAs including flow rates of the carrier fluid transporting the diluting plug, the number of loops and stationary drops, the volume of the diluting plug and stationary drops, and finally the number of diluting plugs. In this work, we keep the ratio of oil flow rate pushing the diluting plug (Q_D) and the oil flow rate for fragmenting the gradient plug (Q_F) fixed at 0.6 to maintain the same droplet size. We also fix the number of loops to be ten and the total length of the bypass channels to be 2.03 cm in all experiments to maintain the same residence time for a given volume of diluting plug. Thus, we specifically investigate the effect of carrier fluid flow rate delivering the diluting plug, volume of diluting plugs, number of diluting plugs, and the volume of stationary sample drops on the dilution range afforded in MDAs. Figure 2A tabulates the explored values for these parameters.

Our findings indicate that increasing the carrier fluid flow rate by an order of magnitude produces only a 2-fold increase in dilution. In contrast, increasing the volume of the diluting plug by a factor of 2 yields about an 8-fold increase in dilution. Likewise, decreasing the stored sample volume by a factor of 5 generates at least a 30-fold increase in dilution. To further increase the volume of diluting plug, without resorting to extremely long plugs, an alternative means is to inject multiple shorter oil-isolated plugs in a single-step through the cartridge. We find that a ∼400-fold span in dilution can be obtained by injecting four, 1 μL water plugs, separated by 1 μL of oil, at flow rate of 60 μL/h (seeing Figure S2, Supporting Information). By injecting even more diluting plugs than demonstrated here, we expect a much wider range of dilution can be detected by

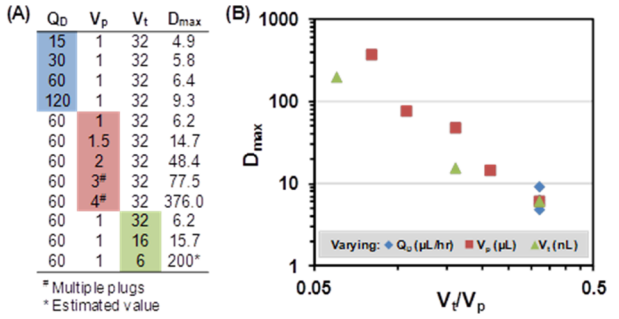

Q_D	V_p	V_t	D_{max}
15	1	32	4.9
30	1	32	5.8
60	1	32	6.4
120	1	32	9.3
60	1	32	6.2
60	1.5	32	14.7
60	2	32	48.4
60	3#	32	77.5
60	4#	32	376.0
60	1	32	6.2
60	1	16	15.7
60	1	6	200*

Multiple plugs
* Estimated value

Figure 2. Parametric investigation of the effect of system parameters on dilution range in the MDA. (A) The list of experimental parameters and the range of their values explored. (B) Plot of the maximum dilution fold (D_{max}) versus the ratio of trap volume (V_t) to plug volume (V_p).

integrating detectors with lower detection limit and higher dynamic range.

We find that an interesting outcome of this parametric investigation is that the volume of diluting plug (V_p) and the volume of trapped drop (V_t) appear to be the key parameters controlling dilution range in the MDA. To further support this claim, we plot, in Figure 2B, the values of D_{max} as a function of the ratio V_t/V_p, collected from all the conditions reported in Figure 2A. We observe a good correlation between the two parameters, indicating that indeed V_t/V_p is an important factor governing the maximum dilution fold. Thus, our microfluidic technique for dilution is similar to performing dilution on the macroscale using pipettes, where the final dilution is simply dictated by the ratio of volumes of sample and buffer. The reason that flow rate has less effect on the dilution is because the mass transfer between the sample drop and diluting plug is much less effective during the advection period. Thus, even though changing the flow rates varies the residence time (0.5−4 min), it does not affect dilution fold. However, the actual shape of the concentration gradient profile may change as the experimental parameters (including flow rate) vary.

We also assessed other performance indicators of our technique such as throughput and repeatability. We find that, at a Q_D of 120 μL/h, it takes 53 s for generating a 1 μL gradient plug and 96 droplets resulting in a throughput of about 6500 drops per hour. We investigated the repeatability of our method by comparing three runs of experiments (separated by a duration of 6 h) at Q_D = 60 μL/h, using a 1 μL diluting plug in the same device (450 μm diameter traps). The plot for the three trials is shown in Supporting Information (Figure S3). The relative standard deviation (RSD) of gray values for the corresponding droplets in the three trials was found to be less than 2%, indicating that the concentration gradients are very reproducible.

Enzyme Inhibition Assay. To address the suitability of our method for biological assays, we applied it to generate a dose-response curve for an enzyme inhibition assay. It is well-known that enzyme β-galactosidase (β-Gal) acts on substrate fluorescein di(β-D-galactopyranoside) (FDG) producing fluorescein. We tested the inhibition activity of diethylenetriaminepentaacetic acid (DTPA) to β-Gal, thus impeding the conversion of FDG to fluorescein. In the experiment, a 200 nL, 5 mM DTPA plug was captured in a SDA with trap size of 320 μm. The concentration gradient of DTPA was produced by diluting the SDA with a 1.5 μL buffer plug. The gradient plug merged with β-Gal and FDG in a volume ratio of 2:1:1 before

dx.doi.org/10.1021/ac303526y | Anal. Chem. 2013, 85, 2044−2048

the fragmentation into droplets, which contains fixed concentrations of enzyme/substrate and gradually decreases concentrations of inhibitor in each drop. The fluorescence intensities of the droplets were measured under a 10× objective after a 15 min incubation at room temperature. The higher the intensity of fluorescence, the lower is the concentration of inhibitor in the droplet and the lower is the inhibition to the enzyme reaction. The concentration of DTPA in each drop was calibrated according to the concentration profile shown in Figure S4B, Supporting Information. A dose-response curve in the range of 0−3 mM DTPA was obtained by defining the fluorescence intensity of 0 mM DTPA to be 100% (i.e., 0% inhibition), as shown in Figure 3. The IC_{50} value deduced from this curve is 0.17 mM DTPA, which is close to the result reported recently.[12]

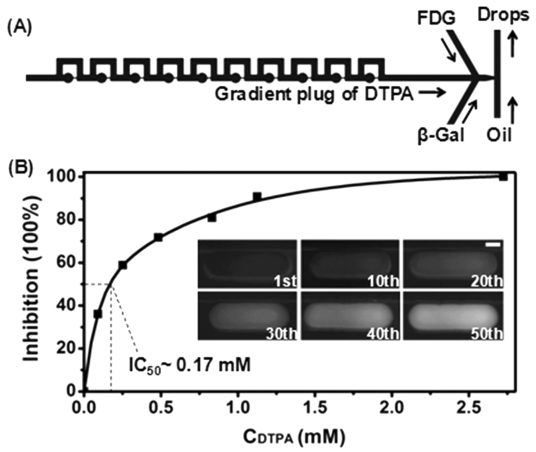

Figure 3. Enzyme inhibition assay. (A) Microfluidic network design showing the gradient generation and reagent merging zones for performing the enzyme inhibition assay. (B) Dose response curve showing inhibition of enzyme β-Gal by DTPA. The curve is derived from data sets of relative fluorescence intensity and concentration calibration of DTPA in each of the droplets (see Figure S4, Supporting Information). Flow rates of diluting plug, FDG, and β-Gal are 30, 15, and 15 μL/h. Q_F = 80 μL/h. Inset images: selected droplets contain decreasing concentration of DTPA. Numbers indicate the sequence of droplets in the array. Scale bar: 100 μm.

Potential for Screening a Library of Compounds. To further demonstrate the potential of our method for high throughput screening, we conducted experiments in which, instead of one sample, dilutions can be performed on multiple samples consecutively. The basic idea behind multiple sample dilution is to remove the static drops containing remnants of the diluted sample by modulating the oil flow rate and feed in new samples and diluting plugs prestored in the cartridge.

In our microfluidic network, sample droplets are immobilized in the fluidic traps when the Laplace pressure drop is higher than the carrier fluid pressure gradient across the droplet; otherwise, the drops would squeeze out of the traps.[19] Thus, previously diluted sample drops can be removed by increasing Q_D[36] above the limit for squeeze-through, as shown in Figure 4A (also in Movie S2 (ac303526y_si_003.avi), Supporting Information), where ten, 16 nL drops are eluted (or removed) out of the 320 μm traps at a flow rate of 30 μL/min in less than 10 s. Repeated experiments showed that traps are emptied within a time interval of 4−9 s. After the traps are emptied, another different sample can be loaded and diluted. Therefore, multiple samples can be tested sequentially by introducing

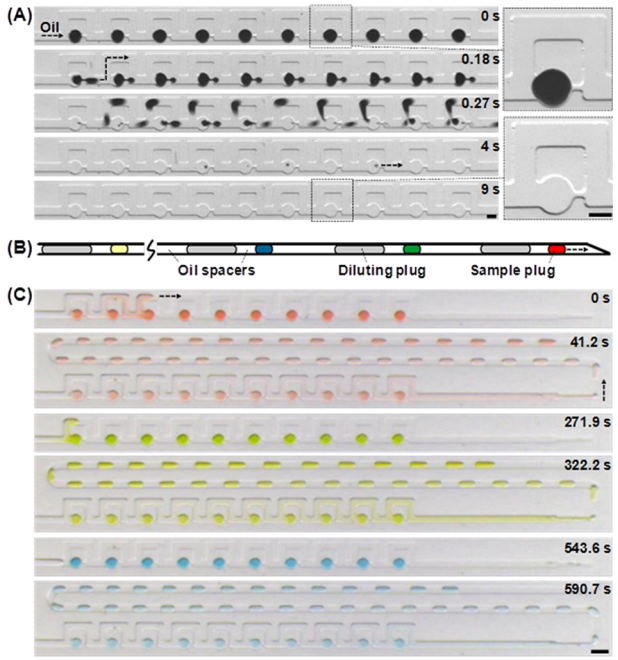

Figure 4. Illustration of sequential dilution of multiple samples. (A) Replacement of an existing sample by modulation of flow rate. Time elapsed images showing drops of black dye squeezing through the traps as the flow rate of pushing oil increased to 30 μL/min. Scale bar: 200 μm. (B) Schematic drawing of sample preparation in cartridge: each sample is followed by a diluting water plug (not to scale). (C) Snap shots of generating concentration gradients of red, green, and blue samples in a sequential fashion. Volumes of sample and diluting plugs are 0.3 and 1.5 μL. Volumes of oil spacers between sample and diluting plugs, between sample pairs, are 1 and 6 μL. Residues of previous sample in the traps are removed by increasing flow rate to 30 μL/min for 10 s. Sample and diluting plugs are flowing at 60 μL/h and Q_F = 100 μL/h. Scale bar: 500 μm. Trap size is 320 μm. Arrows indicate flow direction.

sample plugs followed by diluting plugs with calculated volume of oil spacers for elution and using a programmable pump to switch between the sample injection/dilution flow rate and the elution flow rate. Figure 4B,C and Movie S3 (ac303526y_si_004.avi, Supporting Information), show the concept and three concentration gradients of different species generated in a row, demonstrating the feasibility of this technique for testing multiple samples at varying concentrations.

CONCLUSIONS

We report a new method to generate arrays of droplets with gradual variation in chemical concentrations from drop-to-drop by fragmentation of long immiscible diluting plugs. We show that the dilution range can be tuned by a variety of factors including flow conditions, plug volume, and trap size, which provides flexible control over the concentration gradients achievable in MDAs. Among these factors, however, the maximum dilution fold is strongly a function of the ratio of the volumes of trapped drops and diluting plugs. Smaller trapped volumes and larger volumes (or multiple number) of diluting plugs yield a broader dilution range. We demonstrated a throughput of generating 6500, 10 nL droplets per hour with a fine resolution of variation in chemical concentrations using less than 300 nL of sample; even more higher throughput could be achieved by optimizing the fragmentation flow rate and

dx.doi.org/10.1021/ac303526y | Anal. Chem. 2013, 85, 2044−2048

further downscaling of droplet volumes into picoliter regime. Additionally, the concentration gradients preserved into the MDAs can be manipulated downstream by merging with another stream or drops containing target species. With the demonstrated ability of loading, replacing, and diluting multiple samples on-chip, we believe our microfluidic approach can serve as an inexpensive, low-consumption, and high-throughput screening alternative to robot-aided fluid dilution in multiwell plates.

■ ASSOCIATED CONTENT

Supporting Information

Additional information as noted in text. This material is available free of charge via the Internet at http://pubs.acs.org.

■ AUTHOR INFORMATION

Corresponding Author

*E-mail: meng.sun@ttu.edu (M.S.); siva.vanapalli@ttu.edu (S.A.V).

Notes

The authors declare no competing financial interest.

■ ACKNOWLEDGMENTS

We acknowledge National Science Foundation (CAREER: Grant No. 1150836) for partially supporting this work. M.S. was partially supported by an AFRI grant (Grant No. 2009-02400) from USDA. We thank Zeina S. Khan and Dali Wei for MATLAB tutorial on image analysis.

■ REFERENCES

(1) Song, H.; Chen, D. L.; Ismagilov, R. F. *Angew. Chem., Int. Ed.* **2006**, *45*, 7336−7356.
(2) Teh, S. Y.; Lin, R.; Hung, L. H.; Lee, A. P. *Lab Chip* **2008**, *8*, 198−220.
(3) Chiu, D. T.; Lorenz, R. M.; Jeffries, G. D. M. *Anal. Chem.* **2009**, *81*, 5111−5118.
(4) Theberge, A. B.; Courtois, F.; Schaerli, Y.; Fischlechner, M.; Abell, C.; Hollfelder, F.; Huck, W. T. S. *Angew. Chem., Int. Ed.* **2010**, *49*, 5846−5868.
(5) Pompano, R. R.; Liu, W. S.; Du, W. B.; Ismagilov, R. F. *Annu. Rev. Anal. Chem.* **2011**, *4*, 59−81.
(6) Li, L.; Mustafi, D.; Fu, Q.; Tereshko, V.; Chen, D. L. L.; Tice, J. D.; Ismagilov, R. F. *Proc. Natl. Acad. Sci. U. S. A.* **2006**, *103*, 19243−19248.
(7) Gerdts, C. J.; Elliott, M.; Lovell, S.; Mixon, M. B.; Napuli, A. J.; Staker, B. L.; Nollert, P.; Stewart, L. *Acta Crystallogr., Sect. D: Biol. Crystallogr.* **2008**, *64*, 1116−1122.
(8) Du, W. B.; Sun, M.; Gu, S. Q.; Zhu, Y.; Fang, Q. *Anal. Chem.* **2010**, *82*, 9941−9947.
(9) Song, H.; Ismagilov, R. F. *J. Am. Chem. Soc.* **2003**, *125*, 14613−14619.
(10) Bui, M. P. N.; Li, C. A.; Han, K. N.; Choo, J.; Lee, E. K.; Seong, G. H. *Anal. Chem.* **2011**, *83*, 1603−1608.
(11) Miller, O. J.; El Harrak, A.; Mangeat, T.; Baret, J. C.; Frenz, L.; El Debs, B.; Mayot, E.; Samuels, M. L.; Rooney, E. K.; Dieu, P.; Galvan, M.; Link, D. R.; Griffiths, A. D. *Proc. Natl. Acad. Sci. U. S. A.* **2012**, *109*, 378−383.
(12) Cai, L. F.; Zhu, Y.; Du, G. S.; Fang, Q. *Anal. Chem.* **2012**, *84*, 446−452.
(13) Barbulovic-Nad, I.; Yang, H.; Park, P. S.; Wheeler, A. R. *Lab Chip* **2008**, *8*, 519−526.
(14) Yu, L. F.; Chen, M. C. W.; Cheung, K. C. *Lab Chip* **2010**, *10*, 2424−2432.
(15) Brouzes, E.; Medkova, M.; Savenelli, N.; Marran, D.; Twardowski, M.; Hutchison, J. B.; Rothberg, J. M.; Link, D. R.; Perrimon, N.; Samuels, M. L. *Proc. Natl. Acad. Sci. U. S. A.* **2009**, *106*, 14195−14200.
(16) Du, W. B.; Li, L.; Nichols, K. P.; Ismagilov, R. F. *Lab Chip* **2009**, *9*, 2286−2292.
(17) Selimović, Š.; Gobeaux, F.; Fraden, S. *Lab Chip* **2010**, *10*, 1696−1699.
(18) Fradet, E.; McDougall, C.; Abbyad, P.; Dangla, R.; McGloin, D.; Baroud, C. N. *Lab Chip* **2011**, *11*, 4228−4234.
(19) Sun, M.; Bithi, S. S.; Vanapalli, S. A. *Lab Chip* **2011**, *11*, 3949−3952.
(20) Jeon, N. L.; Dertinger, S. K. W.; Chiu, D. T.; Choi, I. S.; Stroock, A. D.; Whitesides, G. M. *Langmuir* **2000**, *16*, 8311−8316.
(21) Lee, K.; Kim, C.; Ahn, B.; Panchapakesan, R.; Full, A. R.; Nordee, L.; Kang, J. Y.; Oh, K. W. *Lab Chip* **2009**, *9*, 709−717.
(22) Lorenz, R. M.; Fiorini, G. S.; Jeffries, G. D. M.; Lim, D. S. W.; He, M. Y.; Chiu, D. T. *Anal. Chim. Acta* **2008**, *630*, 124−130.
(23) Damean, N.; Olguin, L. F.; Hollfelder, F.; Abell, C.; Huck, W. T. S. *Lab Chip* **2009**, *9*, 1707−1713.
(24) Edgar, J. S.; Milne, G.; Zhao, Y. Q.; Pabbati, C. P.; Lim, D. S. W.; Chiu, D. T. *Angew. Chem., Int. Ed.* **2009**, *48*, 2719−2722.
(25) Theberge, A. B.; Whyte, G.; Huck, W. T. S. *Anal. Chem.* **2010**, *82*, 3449−3453.
(26) Kim, J. Y.; Cho, S. W.; Kang, D. K.; Edel, J. B.; Chang, S. I.; deMello, A. J.; O'Hare, D. *Chem. Commun.* **2012**, *48*, 9144−9146.
(27) Jambovane, S.; Kim, D. J.; Duin, E. C.; Kim, S. K.; Hong, J. W. *Anal. Chem.* **2011**, *83*, 3358−3364.
(28) Churski, K.; Kaminski, T. S.; Jakiela, S.; Kamysz, W.; Baranska-Rybak, W.; Weibel, D. B.; Garstecki, P. *Lab Chip* **2012**, *12*, 1629−1637.
(29) Leung, K.; Zahn, H.; Leaver, T.; Konwar, K. M.; Hanson, N. W.; Page, A. P.; Lo, C. C.; Chain, P. S.; Hallam, S. J.; Hansen, C. L. *Proc. Natl. Acad. Sci. U. S. A.* **2012**, *109*, 7665−7670.
(30) Niu, X. Z.; Gielen, F.; Edel, J. B.; deMello, A. J. *Nat. Chem.* **2011**, *3*, 437−442.
(31) Bithi, S. S.; Vanapalli, S. A. *Biomicrofluidics* **2010**, *4*, 044110-1−044110-10.
(32) Boukellal, H.; Selimović, Š.; Jia, Y. W.; Cristobal, G.; Fraden, S. *Lab Chip* **2009**, *9*, 331−338.
(33) Shestopalov, I.; Tice, J. D.; Ismagilov, R. F. *Lab Chip* **2004**, *4*, 316−321.
(34) Abate, A. R.; Hung, T.; Mary, P.; Agresti, J. J.; Weitz, D. A. *Proc. Natl. Acad. Sci. U. S. A.* **2010**, *107*, 19163−19166.
(35) Frenz, L.; El Harrak, A.; Pauly, M.; Bégin-Colin, S.; Griffiths, A. D.; Baret, J. C. *Angew. Chem., Int. Ed.* **2008**, *47*, 6817−6820.
(36) Cohen, D. E.; Schneider, T.; Wang, M.; Chiu, D. T. *Anal. Chem.* **2010**, *82*, 5707−5717.